Beryllium-boron systematics of two distinctive CAIs from CV3 chondrites: the relatively pristine CAI B4 from NWA 6991 and the FUN CAI CMS-1 from Allende. E. Dunham[1,2], M. Wadhwa[1,2], S. J. Desch[2]. [1]Center for Meteorite Studies, [2]School of Earth and Space Exploration, Arizona State University, Tempe, AZ 85287 (etdunham@asu.edu)

Introduction: Beryllium-10, which decays to ^{10}B with a half-life of 1.4 Ma, is produced almost exclusively by irradiation reactions induced by solar or galactic cosmic rays ([1], and references therein). Previous studies have demonstrated that primitive Calcium-Aluminum-rich Inclusions (CAIs) in several carbonaceous chondrite types record the prior existence of this short-lived radionuclide, with an initial $^{10}Be/^{9}Be$ ratio in the range of $\sim10^{-4}$-10^{-2} [2-8]. These findings have important implications for understanding the astrophysical birth environment of our Solar System [1].

There are two possible astrophysical settings in which the ^{10}Be in the early Solar System may have originated. One possible setting is the dense protosolar molecular cloud core where ^{10}Be may have been enhanced by trapping of galactic cosmic rays [9] or by spallogenesis during energetic particle irradiation [2]. An alternative setting is within the solar nebula, where irradiation of gas and/or refractory solids during an early active phase of the Sun may have produced ^{10}Be [2,10,11]. In this setting, local irradiation could have produced significant temporal and spatial variations in ^{10}Be abundances. Thus far, the wide range in the initial $^{10}Be/^{9}Be$ ratio inferred from previous studies [2-8] appears to be more consistent with the latter.

In this study we report the $^{10}Be/^{9}Be$ ratios of two well-studied CAIs, B4 from the NWA 6991 CV3 chondrite and CMS-1 FUN inclusion from the Allende CV3 chondrite, and predict that ^{10}Be was formed by irradiation within the hot solar nebula accretion disk.

Samples: The B4 inclusion is a relatively pristine Compact Type A (CTA) CAI from the $CV3_{ox}$ chondrite NWA 6991 [12-14]. The melilite grains are coarse (up to 1 mm diameter) and are primarily gehlinitic with $\sim Åk_{4\text{-}61}$; secondary alteration is only a minor component of B4 [14]. This inclusion has an ancient absolute Pb-Pb age of 4567.94 ± 0.31 Ma [12]. Furthermore, it has well-behaved Al-Mg systematics corresponding to a near-canonical $^{26}Al/^{27}Al$ ratio [13].

The CMS-1 inclusion from the $CV3_{ox}$ chondrite Allende is a CAI with FUN (Fractionation and Unidentified Nuclear) effects [15,16]. It is an irregularly shaped CTA composed mainly of pyroxene and melilite ($\sim Åk_{18\text{-}48}$) with abundant spinel inclusions. It was identified as a FUN CAI because it is characterized by large nucleosynthetic anomalies in titanium [17] and mass-dependent fractionations in oxygen, magnesium and silicon isotopes [15]. As is the case for other FUN CAIs, CMS-1 has an initial $^{26}Al/^{27}Al$ that is significantly lower than the canonical value commonly seen in normal CAIs [15]. We note that Be-B systematics have been previously determined in only two other FUN CAIs [4,7].

Analytical Methods: Polished thin sections of each of the two CAIs studied here were thoroughly cleaned with mannitol (ultrasonication and soaking) to remove surface boron contamination. Analyses of the B isotopic composition and the Be/B ratios were performed using the Cameca IMS-6f secondary ion mass spectrometer (SIMS) at Arizona State University (ASU). A focused $^{16}O^-$ primary beam was tuned to produce a 20-30 μm diameter spot with primary ion intensity of 10-20 nA. We performed Be-B analyses primarily on melilite since it is the major carrier of Be in CAIs and typically has higher Be/B ratios than other phases in refractory inclusions [3,5]. Our analysis spots on the melilites in each CAI were chosen based on backscattered electron images to avoid possible cracks and fine inclusions. We operated the mass spectrometer at a mass resolving power of ~1000 to resolve and avoid hydride, Al^{3+}, and Si^{3+} interferences. We measured $^{9}Be^+$ (8s), $^{10}B^+$ (16s) and $^{11}B^+$ (4s) for 20 to 150 cycles for each measurement. At the end of each analysis, $^{28}Si+$ was additionally measured; the measured (B^+ or Be^+)/Si^+ ratios were used, along with the standard measurements, to determine Be and B concentrations. The IMt-1 clay standard was used to correct for instrumental mass fractionation of B isotopes, whereas the NIST610 glass was used for obtaining the relative sensitivity factor (RSF) for the calculation of Be/B ratios. Following SIMS analyses of the CAIs, the SIMS spots were examined with a JEOL JXA-8520F electron microprobe at ASU; data from spots which were located on cracks were excluded from the isochron regression.

It was shown recently that for an accurate quantification of the Be/B ratios in melilite via SIMS analyses, the RSF needs to be determined using melilite composition glass standards [18]. We are currently in the process of synthesizing several melilite composition glasses (with a range of Be/B ratios) by melting mixtures of oxide powders in a DelTech furnace in the Depths of the Earth Laboratory at ASU. The major element concentrations in these glasses will be determined using the JEOL JXA-8520F electron microprobe at ASU, while Be and B concentrations will be measured using the Thermo ICAP-Q ICPMS at ASU (following the procedures of [19]). Using these glasses,

we plan to determine the RSF for the calculation of Be/B ratios for melilites with the Cameca IMS-6f SIMS at ASU in the near future. However, in the meantime, the absolute values of the $^{10}Be/^{9}Be$ ratios inferred here may be inaccurate (by a small, but as yet undetermined, factor; for example, [18] noted that the RSF, $(^{9}Be^{+}/^{11}B^{+})/(^{9}Be/^{11}B)$, for their Cameca NanoSIMS instrument using the NIST610 glass standard was ~16% higher than for melilite-like glass standards). Nevertheless, the relative differences between the $^{10}Be/^{9}Be$ ratios inferred for the two CAIs in this study as well as those analyzed previously by us [20, 21] are likely to be robust.

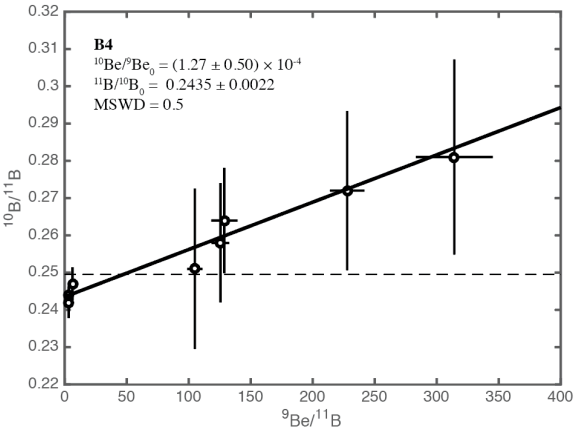

Figure 1: Be-B isochron diagram for melilite in B4 CAI from NWA 6991. The horizontal dashed line represents the chondritic value of $^{10}B/^{11}B$ (=0.2481; [27]). The error bars are 2 sigma, calculated from counting statistics.

Results: Figure 1 shows a Be-B isochron plot for the B4 CAI from NWA 6991. The data define a slope corresponding to a $^{10}Be/^{9}Be$ ratio of $(1.27 \pm 0.50) \times 10^{-4}$ (MSWD = 0.5) and an initial $^{10}B/^{11}B$ ratio of 0.2435 ± 0.0022. The melilites analyzed in the FUN CAI CMS-1 from Allende had relatively low $^{9}Be/^{11}B$ ratios (<~30). As such, we could only infer an upper limit on the $^{10}Be/^{9}Be$ ratio of 5.8×10^{-4} for this inclusion; it has an initial $^{10}B/^{11}B$ ratio of 0.2501 ± 0.0072.

Discussion: The B4 CAI records the lowest well-resolved $^{10}Be/^{9}Be$ ratio found so far. Since this CAI is thought to be relatively undisturbed [12-14], this ^{10}Be abundance is likely to be the inherent value for this CAI, unaffected by secondary processing. This low ratio further widens the range of $^{10}Be/^{9}Be$ ratios that we have previously reported in other relatively pristine CAIs [20,21] and further indicates that the predominant source of ^{10}Be was local irradiation within the solar nebula. In this context, it is important to note that this CAI has an ancient Pb-Pb age, and a near-canonical initial $^{26}Al/^{27}Al$ ratio; we suggest the low ^{10}Be abundance in B4 could represent a baseline level present in material inherited from the molecular cloud.

It is additionally interesting to note that the $^{10}Be/^{9}Be$ ratios inferred for two previously analyzed FUN CAIs [4,7] fall within the range of $^{10}Be/^{9}Be$ ratios we have reported thus far for relatively pristine normal CAIs [20,21]. Furthermore, the initial $^{10}B/^{11}B$ ratios for these FUN CAIs, as well as for the FUN CAI CMS-1 analyzed here, are the same within the errors as those for these normal CAIs. This suggests that ^{10}Be in FUN and normal CAIs originated in the same mechanism/environment.

Finally, we propose a new model in which much of the ^{10}Be inferred to be present in CAIs originated locally in the solar protoplanetary disk. Specifically, we propose that energetic particles generated by magnetic turbulence near the midplane of the disk induce nuclear reactions that lead to production of the short-lived radionuclides ^{10}Be and ^{36}Cl (half-life ~0.3 Ma). [22] also argued that energetic particles would be generated by magnetic reconnection events due to magnetic turbulence, but they focused only on the ability of those particles to ionize gas, and considered only turbulence in the low-density corona of the disk, whereas we investigate the ability of particles to induce nuclear reactions at the dense midplane of the disk. Magnetic turbulence due to the magnetorotational instability requires high temperatures to ionize the gas, but the high midplane temperatures associated with CAI formation are sufficient to produce free electrons and K and Na ions [23]. The range of $^{10}Be/^{9}Be$ ratios observed in the earliest formed Solar System solids is ~ $(1–10) \times 10^{-4}$ [this work, 2-8,20,21] while $^{36}Cl/^{35}Cl$ ratios in these objects are ~10^{-5}–10^{-6} [24-26]. We will present calculations testing whether these abundances can be simultaneously produced by the energetic particles produced by magnetic turbulence at the disk midplane.

References: [1] Davis A.M. & McKeegan K.D. (2014), *Treatise on Geochemistry (2nd Ed.),* p.361. [2] McKeegan K. et al. (2000) *Science 289,* 1334. [3] Sugiura N. et al. (2001) *MAPS 36,* 1397. [4] MacPherson G. et al. (2003) *GCA 67,* 3165. [5] Chaussidon M. et al. (2006) *GCA 70,* 224. [6] Liu M.-C. et al. (2009) *GCA 73,* 5051. [7] Wielandt D. et al. (2012) *ApJ 748,* 25. [8] Gounelle M. et al. (2013) *ApJ 763,* 33. [9] Desch S. et al. (2004) *ApJ 602*, 528. [10] Gounelle M. et al. (2001) *ApJ 548,* 1051. [11] Bricker G. & Caffee M. (2010) *ApJ 725,* 443. [12] Bouvier, A. et al. (2011) *Workshop on Formation of the First Solar System Solids,* Abstract #9054. [13] Wadhwa, M. et al. (2014) *LPS 45,* Abstract #2698. [14] Bullock E. et al. (2014) *LPS 45,* Abstract #1919. [15] Williams C.D. et al. (2016) *GCA*, in press. [16] Mendybaev R.A. et al. (2016) *GCA*, in press. [17] Williams C.D. et al. (2012) *LPS* Abstract #2523. [18] Fukuda K. et al. (2016) *MetSoc* Abstract #6459. [19] Gangjian W. et al. (2013) *Anal. At. Spectrom. 28*, 606. [20] Dunham E. et al. (2016) *LPS 47,* Abstract #2723. [21] Dunham E. et al. (2016) *MetSoc* Abstract #6222. [22] Turner N.J. & Drake J.F. (2009) *ApJ 703,* 2152. [23] Desch S.J. & Turner N.J. (2015) *ApJ 811,* 156. [24] Jacobsen B. et al. (2011) *ApJ 731*, 28. [25] Lin Y. et al. (2005) *PNAS 102*, 1306. [26] Hsu W. et al. (2006) *ApJ 640*, 525. [27] Zhai M. et al. (1996) *GCA 60*, 4877.